FISEVIER

Contents lists available at ScienceDirect

Journal of the European Ceramic Society

journal homepage: www.elsevier.com/locate/jeurceramsoc



Original Article

Comparison of traditional and flash pyrolysis of different carbon content silicon oxycarbides



Kathy Lu*, Donald Erb, Kaustubh Bawane, Ni Yang

Department of Materials Science and Engineering, Virginia Polytechnic Institute and State University, Blacksburg, VA, 24061, USA

ARTICLE INFO

Keywords:
Silicon oxycarbide
Flash pyrolysis
Free carbon
Phase content
Gibbs free energy minimization

ABSTRACT

This study is to understand the effect of carbon content on the pyrolysis behaviors and phase contents of silicon oxycarbides (SiOCs). Flash pyrolysis conditions, evolution of different SiOC phases, and free carbon types/amounts are compared for C-rich and less C-rich precursors. The C-rich system experiences the flash event at a much lower pyrolysis temperature with a much higher current density even though the internal temperatures at flash are very similar. SiC formation is more obvious for the C-rich samples along with a much higher carbon content under both flash and traditional pyrolysis conditions. The phase contents of SiO₂, SiC, and other SiOC intermediates can be calculated using a Gibbs energy minimization method, showing that the C-rich sample has more C-rich SiOC intermediates while the less C-rich sample has more Si-rich intermediates. This research provides a general framework in assessing the pyrolysis behaviors of different SiOC materials.

1. Introduction

Polymer derived ceramics, such as SiOC, SiCN, and SiBCN, are important materials with excellent mechanical properties, high temperature stability, and corrosion resistance [1–4]. Traditional processing of polymer derived ceramics begins with a polymer precursor, which is heated in an inert atmosphere for pyrolysis and conversion to ceramics. The most extensively studied systems are related to silicon oxycarbide (SiOC) derived from polysiloxanes [5–11]. At low pyrolysis temperatures (800 °C–1100 °C), the ceramic is composed of an amorphous SiOC phase, in which Si is tetrahedrally bonded to either oxygen or carbon to form SiO_xC_{4-x} bonds, as well as a disordered "free carbon" phase, depending on the starting polymer composition [10,12,13]. At temperatures greater than ~1250 °C, the SiOC phase partially phase separates, forming SiO_2 nanodomains, SiC crystallites, and additional free carbon [12–18].

From a different perspective, traditional processing of bulk ceramics involves sintering of a starting powder material. A new field-assisted technique, termed flash sintering, was first reported in 2010 [19]. By applying a constant electric field during heating, this process can densify samples in short periods of time at furnace temperatures significantly lower than those required in conventional sintering [19]. During the flash event, the electrical conductivity of the sample experiences a sharp nonlinear increase, resulting in sample heating to several hundred degrees Celsius higher than the furnace temperature

due to Joule heating. Flash sintering has been conducted for numerous ceramic materials such as yttrium-stabilized zirconia, magnesia-doped alumina, strontium titanate, and cobalt manganese oxide [19–25].

Recently, the same processing ideology behind flash sintering was applied to polymer derived ceramics for the first time [26,27]. This process was termed flash pyrolysis since it involves conversion of a bulk polymer precursor into a ceramic rather than sintering of a powder material under an applied electric field. The results of using flash pyrolysis at temperatures as low as 780 °C show that the onset of the flash event is dependent on the nucleation of the free carbon phase. Additionally, the samples that are flashed with an electric field between 30-50 V/mm have a more ordered free carbon phase compared to the samples pyrolyzed at 1300 °C without an electric field [26]. The ordering of the carbon phase with an applied electric field is attributed to the simultaneous Joule heating and electromigration, which is the collision of electrons/holes and defects [28]. The coupled Joule heating and electromigration cause a faster flux of defects out of the carbon lattice, allowing for more complete ordering of the free carbon phase [26]. Such carbon ordering, e.g., formation of graphene-like and turbostratic carbon, has also been observed for spark plasma sintered SiOC whereas no graphene is found at the same temperature without an electric field [29,30].

However, many questions still remain about flash pyrolysis of polymer derived ceramics. Microstructure evolution and compositional differences of SiOCs from polymer precursors of different amount of

^{*} Corresponding author.

E-mail address: klu@vt.edu (K. Lu).

carbon are especially important. The phase separation differences in SiOCs from traditional pyrolysis and flash pyrolysis remain to be evaluated. For flash sintering, the starting powder materials are often already in a stable state, no significant mass loss or atomic level structural reorganization is expected. Sintering mostly occurs through diffusion-induced densification and grain growth. For polymer derived ceramics such as SiOCs, radical species can continuously evolve at high temperatures; new phase formation and existing phase evolution are simultaneous events; up to 40% mass loss and up to 56% volume shrinkage can occur [31,32]. The effects of free carbon and carbon ordering on the phase development of SiOCs remain to be addressed during the drastic ceramic formation process. Carbon dictates the electrical conductivity of the samples and thus the flash pyrolysis degree and should be further evaluated. In addition, phase contents of different SiOC intermediates have never been quantified for SiOCs.

In this study, flash pyrolysis and traditional pyrolysis were studied using polysiloxane precursors, one of a high carbon content (PMPS) and one of a low carbon content (Tospearl). The effects of the flash pyrolysis characteristics, the carbon content on the SiOC phase evolution, and the evolution of the free carbon in the SiOCs were investigated in order to understand and predict the fundamental changes in the SiOC microstructures. A Gibbs free energy minimization method was used to predict the phase contents in the resulting SiOCs.

2. Experimental procedures

In this work, the C-rich polymer precursor was composed of vinylterminated polymethylphenylsiloxane (PMPS, $[Si(CH_3)(C_6H_5)O]_n$, Gelest Inc., Morrisville, PA) and polyhydromethylsiloxane (PHMS, $[Si(H)(CH_3)O]_n$, Gelest Inc., Morrisville, PA). 2.1–2.4 wt% platinum-divinyltetramethyldisiloxane complex in xylene (Pt catalyst, Gelest Inc., Morrisville, PA) was used as the crosslinking catalyst for the above polymer precursor mixture. A commercially available polysilsesquioxane pre-crosslinked in a powder format (Tospearl 120, $[Si(CH_3)O_{1.5}]_n$, Momentive Performance Materials Japan Inc., Tokyo, Japan) was used as the low carbon content precursor, which has an average particle size of 2 µm [33], consistent with our own measurement using a transmission electron microscope (JEOL 2100, JEOL USA, Peabody, MA).

The carbon rich polymer precursor was synthesized by first mixing 85 wt% PMPS and 15 wt% PHMS into a solution, followed by sonication for 10 min, and high energy milling (Spex 8000 M Mixer/Mill, Spex Sample Prep, Metuchen, NJ) for 10 min. Then the Pt catalyst (5 ppm relative to PHMS) was added, the mixture was mixed again in the high energy ball mill for 5 min, and then poured into aluminum foil molds. The filled molds were placed into a vacuum chamber and vacuumed for 10 min at 1500 mTorr to remove any bubbles in the mixtures, and then placed in an oven to crosslink at 50°C for 12 h and then at 120°C for 6 h. The samples were referred to as PMPS. The Tospearl polymer precursor powder was used without any further modifications.

Both the PMPS and Tospearl precursors were pyrolyzed to 700 °C before use in order to allow the samples to go through the majority of polymer chain breakup, mass loss, and sample shrinkage. The pyrolyzed powders were then uniaxially pressed at ~500 MPa into disks with diameters of ~1 cm. For the Tospearl powder sample, liquid PHMS was used as a binder; for the pre-pyrolyzed PMPS powder, liquid PMPS was used as a binder. Both liquid binder amounts were 1–2 wt% of the pre-pyrolyzed powder samples. A silver-palladium paste (conductor type 9627, ESL Electro Science, King of Prussia, PA) was applied to the two faces of the pressed samples and dried in order to achieve good electrical contact and serve as electrodes. The samples were then placed into a zirconia crucible and connected to the power supply by platinum wires. A detailed figure showing the flash setup has been given in our prior work [26].

The samples were put into a tube furnace (1730-20 Horizontal Tube Furnace, CM Furnaces Inc., Bloomfield, NJ) and pyrolyzed in argon

with a flow rate of about 70 std cm 3 s $^{-1}$ and a heating rate of 5 °C min $^{-1}$ to 770 °C for PMPS and 1100 °C for Tospearl. Upon reaching the maximum temperature, an electric field was applied. Two commercial DC power sources (Bertan 210-01R Spellman, Hauppauge, NY and FB200 Fisher Scientific) were used to apply a specific voltage to the specimen with a current limit of 2 A, at which the power supply automatically switched to the current control mode. In addition, the PMPS and Tospearl samples were pyrolyzed in Ar without any electric field to 1400 °C at a heating rate of 1°C/min for 2 h as reference samples.

The phase compositions of the pyrolyzed samples were analyzed in an X'Pert PRO diffractometer (PANalytical B.V., EA Almelo, the Netherlands) with Cu K α radiation. Raman spectra were recorded on a Horiba spectrometer (JY Horiba HR 800) with an excitation wavelength of 514 nm produced by an Ar laser between the spectral range of $100\text{--}4000~\text{cm}^{-1}$. The microstructures of the pyrolyzed ceramics were studied using a transmission electron microscope (JEOL 2100, JEOL USA, Peabody, MA); the TEM samples were prepared by grinding in a mortar and then dispersing in absolute ethanol. The compositions of the samples were analyzed by a combustion method for carbon and an ICP-OES method for silicon. Acid digestion and titration were used to obtain the silicon content. The oxygen content was extracted based on the above results and the total mass of the samples. These experiments were conducted by Galbraith Laboratories, Inc. (Knoxville, TN) based on multiple measurements.

The power density P_W (mW/mm³) has been calculated according to the relationship [20]:

$$P_{W} = Ej (1)$$

where j is current density, A /mm². E is electric field, V/mm.

During the flash pyrolysis, the insulating nature of the polymer precursors and decomposed radicals created a state that a large amount of Joule heating was generated. Joule heating caused drastic sample temperature increase. The estimated sample temperature during the flash has been studied based on blackbody radiation using the following equation [23,24,34]:

$$T = T_F \alpha \left[1 + \frac{1000 P_W}{\sigma_{SF} T_F^4} \left(\frac{V}{A} \right) \right]^{\frac{1}{4}}$$
(2)

where T_F is the furnace temperature at the onset of the flash in Kelvin, σ_{SF} is the Stefan-Boltzmann constant with a value of $5.67\times10^{-8}\,\text{Wm}^{-2}\,\text{K}^{-4},\,\alpha$ is a correction factor to account for emissivity less than that expected for a perfect blackbody (approximately 1), V is the volume of the specimen in m^3 , and A is the surface area of the specimen in m^2 .

3. Results and discussion

3.1. Flash pyrolysis characteristics

The changes in electric field, current density, and power density for the PMPS and Tospearl samples as a function of the applied electric field time are shown in Fig. 1. The actual furnace temperatures for the PMPS and Tospearl samples were 770 °C and 1100 °C, respectively. For the flash event to happen, the necessary electric field for the PMPS sample is 40 V/mm for 26 min while it is 100 V/mm for 71 min for the Tospearl sample. Due to the polymer precursor difference, more specifically the carbon content difference in the precursors, the required electrical field for the Tospearl sample is 150% higher and the electric field applied time is 173% longer. This means that a higher driving force for the flash event is needed for the relatively C-poor samples. In addition, the current density at the flash for the PMPS sample increases to 15 mA/mm² in only 26 min while for the Tospearl sample it only increases to 9 mA/mm² in 71 min. The current density in the PMPS sample is 66% higher than that in the Tospearl sample. Because of the electric field (E) and current density (j) difference, according to Eq. (1),

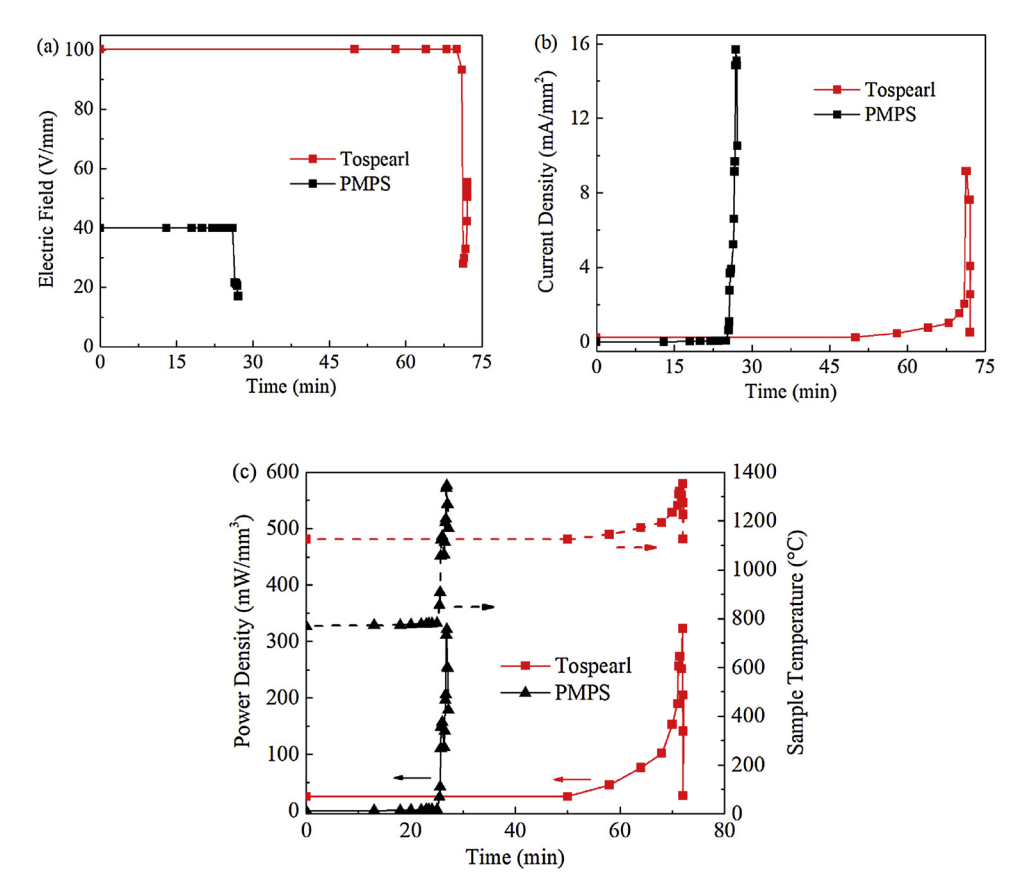


Fig. 1. Changes in electric field (a), current density (b), and power density (c) for the PMPS and Tospearl samples as a function of the applied electric field time.

the difference in power density (P_w) can be calculated as shown in Fig. 1(c) along with the sample internal temperature changes calculated using Eq. (2). The power density for the PMPS sample is $321.7 \, \text{mW/mm}^3$ while for the Tospearl sample it is $323.3 \, \text{mW/mm}^3$. Surprisingly, the power densities in the two kinds of samples are almost the same, a reflection of the similar energies needed for the phase changes.

A more revealing finding is the internal temperature profile difference. For the PMPS sample, the temperature increase is precipitous up to 1345 °C. For the Tospearl sample, following a long incubation period, the temperature change is incremental until it reaches the peak temperature of 1352 °C followed by a sudden drop. This observation indicates that the build-up process for the flash event in the samples with different carbon content is very different. However, the flash event ends at very similar points. The peak temperature for the PMPS sample is 1345 °C and for the Tospearl sample it is 1352 °C, surprisingly very close to each other even though the two systems experience very different furnace temperatures (770 °C vs. 1100 °C). The similar internal temperatures mean that the actual pyrolysis environments in the two kinds of samples are not very different. However, the sudden temperature increase of the PMPS samples leads to sample fracture soon after the flash event while the Tospearl samples stay intact.

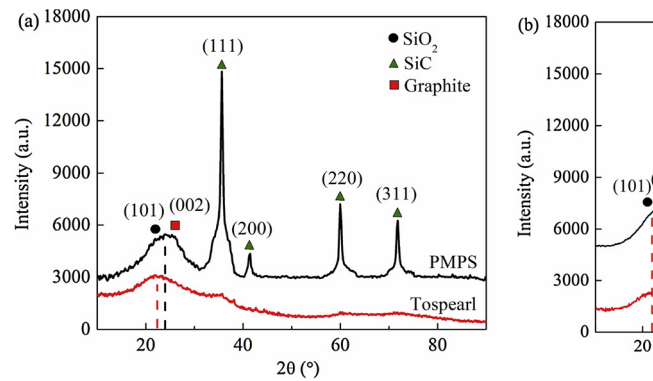
The fundamental difference during the flash pyrolysis for the PMPS and Tospearl samples can be described as follows. At the flash temperature, the pre-pyrolyzed samples are composed of C-containing and Si-containing radicals. With the temperature increase to the flash pyrolysis point, a conductive free carbon phase forms [35] and causes the sudden increases in the current density and power density as well as the sudden drop in the electric field. Since the PMPS sample starts from a C-rich polymer precursor, the carbon phase percolation for the ending of the flash event occurs at a lower temperature and in a much shorter time than that of the less C-rich Tospearl, thus the flash happens at a lower temperature and in a sudden manner. In Fig. 1(b) and (c), the increases in the current density and power density for the PMPS sample

are also much steeper than those for the Tospearl sample, another indication of the quick carbon network formation in the PMPS sample. This can be understood from the point that the C-rich sample has more conductive carbon available for network formation, only a small amount of ordering is required before the conductive network is formed. For the Tospearl sample, the carbon content is low, more time is required before the conductive carbon network forms; this process is also gradual because of the lower degree of carbon ordering as to be shown in Table 2.

3.2. Evolution of SiOC phases

The XRD patterns for the PMPS and Tospearl samples after the flash pyrolysis are shown in Fig. 2(a). The Tospearl sample shows a broad halo peak at ~22° due to the formation of amorphous SiO₂, as well as the tiny, almost invisible peaks at 35.7°, 60.0°, and 71.9° corresponding to the diffraction peaks of crystalline $\beta\text{-SiC}$. The PMPS sample shows a higher intensity halo at ~22.5° along with multiple and well-defined SiC peaks at 35.7°, 41.4°, 60.0°, and 71.9°, corresponding to the (111), (200), (220), and (311) crystalline planes of the β-SiC phase (JCPDS Card No. 01-073-1665). Based on the phase contents in Table 3, even for the flash pyrolyzed PMPS samples, the SiC amount is still very low, at 0.1%. The sharper SiC peaks in Fig. 2(a) may be more related to the SiC crystallite size than the amount. The peak shift from ~22° to ~22.5° indicates graphitic carbon formation for the PMPS sample. Compared to the XRD patterns of the corresponding samples from the traditional pyrolysis at 1400 °C (Fig. 2(b)), the flash pyrolysis can lead to more obvious phase separation at much lower furnace temperatures.

The resulting compositions for the flash pyrolyzed and traditionally pyrolyzed samples are given in Table 1. As seen, the PMPS samples have much higher carbon contents at both pyrolysis conditions, 40.9 wt% after the flash pyrolysis and 45.8 wt% after the traditional pyrolysis. The Tospearl samples are more Si-rich and O-rich, with only 12.3 wt%



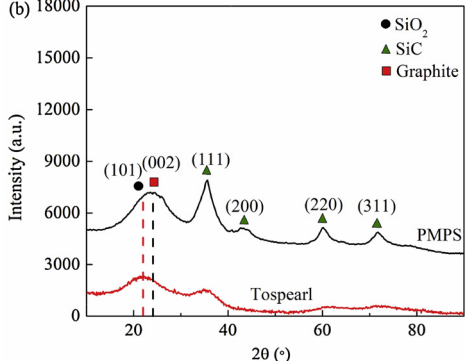


Fig. 2. XRD patterns for the PMPS and Tospearl samples: a) flash pyrolyzed, b) pyrolyzed at 1400 °C without an electric field.

Table 1
SiOC compositions after pyrolysis from different precursors with and without flash.

	C (wt%)	Si (wt%)	O (wt%)
PMPS, flash pyrolysis at 770 °C	40.9	31.5	27.6
Tospearl, flash pyrolysis at 1100 °C	12.3	43.3	44.4
PMPS, traditional pyrolysis at 1400 °C	45.8	32.6	21.6
Tospearl, traditional pyrolysis at 1400 °C	9.7	45.8	44.5

(flash pyrolyzed) and 9.7 wt% (traditional pyrolysis) carbon, respectively. It also shows that the flash pyrolysis leads to a higher carbon retention for the Tospearl sample (increased from 9.7 wt% for the traditional pyrolysis to 12.3 wt% for the flash pyrolysis) but a lower carbon content for the PMPS sample (decreased from 45.8 wt% for the traditional pyrolysis to 40.9 wt% for the flash pyrolysis).

Based on the well-known phase separation reaction for SiOC and carbothermal reaction for SiO₂ (Eqs. (3) and (4)), SiO₂ formation is the pre-condition for SiC formation. Eq. (3) represents the SiOC phase separation into amorphous SiO₂, SiC(β), and graphitic carbon at low pyrolysis temperatures (800–1100°C) [36]. Eq. (4) indicates that carbothermal reaction occurs between SiO₂ and graphite, producing SiC(β) and CO gas at above 1100°C [37]. For the PMPS sample, the C-rich nature is not conducive for SiO₂ formation even though Eq. (4) should proceed more easily. For the Tospearl sample, the free carbon content is low, so Eq. (3) should proceed more easily; however, SiC formation is hindered due to the lack of carbon. The final phase contents are a combined result of these two related processes.

$$2SiOC \rightarrow SiO_2 (amorphous) + C (graphite) + SiC (\beta)$$
 (3)

$$2SiO_2$$
 (amorphous) + $3C$ (graphite) $\rightarrow SiC$ (β) + $2CO$ (g) (4)

As shown in Fig. 3(a), the flash pyrolyzed PMPS sample has a significant amount of free carbon, demonstrated by the graphene layers around the crystallites (shown by the red circles) among an amorphous matrix. For the crystallites, the diffraction pattern on the right side of Fig. 3(a) has separated rings with sparsely distributed bright diffraction spots and the species is identified as $\beta\text{-SiC}$. For the flash pyrolyzed Tospearl sample, Fig. 3(b) shows a largely amorphous structure with mostly SiOC species and possibly the amorphous SiO2 phase; very little

Table 3
Different SiOC phase amounts (mol%) after flash and traditional pyrolysis.

	SiO_2	$SiO_{\frac{3}{2}}C_{\frac{1}{4}}$	$SiOC_{\frac{1}{2}}$	$SiO_{\frac{1}{2}}C_{\frac{3}{4}}$	SiC
PMPS, flash pyrolysis at 770 °C	20.1	16.6	8.5	4.4	0.1
Tospearl, flash pyrolysis at 1100 °C	56.6	20.9	5.1	1.1	0.1
PMPS, traditional pyrolysis at 1400 °C	7.7	12.9	13.1	13.4	0.4
Tospearl, traditional pyrolysis at 1400 °C	52.6	28.7	7.5	0.0	0.4

free carbon can be observed. As a result, the electron diffraction pattern only shows a large halo (right side of Fig. 3(b)) without any diffraction spots. It should also be mentioned that even though the SiC peaks are fairly strong in Fig. 2(a) and (b), the SiC crystallites are mostly buried in the amorphous SiOC matrix and free carbon as shown in Fig. 3(a). For the PMPS sample pyrolyzed using the traditional process to 1400°C, the SiC crystallite size is even smaller as shown in Fig. 3(c) (indicated by the red circles) and there are only two very weak diffraction spots in the diffraction pattern on the right side of Fig. 3(c) (top, between 11-12 o'clock direction). The electron diffraction pattern difference in Fig. 3(a) and (c) is consistent with the XRD diffraction pattern difference in Fig. 2. The SiC nanocrystallite size and crystallinity differences (larger size, better developed crystallinity for the flash pyrolyzed sample) lead to the diffraction pattern difference. For the traditionally pyrolyzed Tospearl sample at 1400 °C, the image and diffraction pattern are very similar to those in Fig. 3(b) and omitted here for brevity.

3.3. Evolution of free carbon

For the PMPS sample, the ceramic yield is 53.4% under the flash pyrolysis condition and 74.5% under traditional pyrolysis at 1400 °C. For the Tospearl sample, the ceramic yield is 89.6% with the flash pyrolysis and 78.9% under traditional pyrolysis at 1400 °C. This means that the polymer to ceramic conversion occurs differently and thus has opposite effects on the ceramic yield. Based on the compositions of the flash pyrolyzed PMPS and Tospearl samples in Table 1, the free carbon phase amount can be calculated from $SiO_aC_b = f_c \cdot C + (1 - f_c) \cdot SiO_xC_y$ and the results are shown in Table 2. For the flash pyrolyzed PMPS sample, it is 50.3 mol%. For the flash pyrolyzed Tospearl sample, it is 16.2 mol%. For the traditionally pyrolyzed PMPS sample, it is 52.6 mol

Table 2Carbon contents after pyrolysis with and without flash for the samples from different precursors.

	Total free carbon content (mol%)	D carbon content (mol%)	G carbon content (mol%)
PMPS, flash pyrolysis at 770 °C	50.3%	36.5%	13.8%
Tospearl, flash pyrolysis at 1100 °C	16.2%	12.9%	3.3%
PMPS, traditional pyrolysis at 1400 °C	52.6%	39.4%	13.3%
Tospearl, traditional pyrolysis at 1400 °C	10.8%	8.8%	2.0%

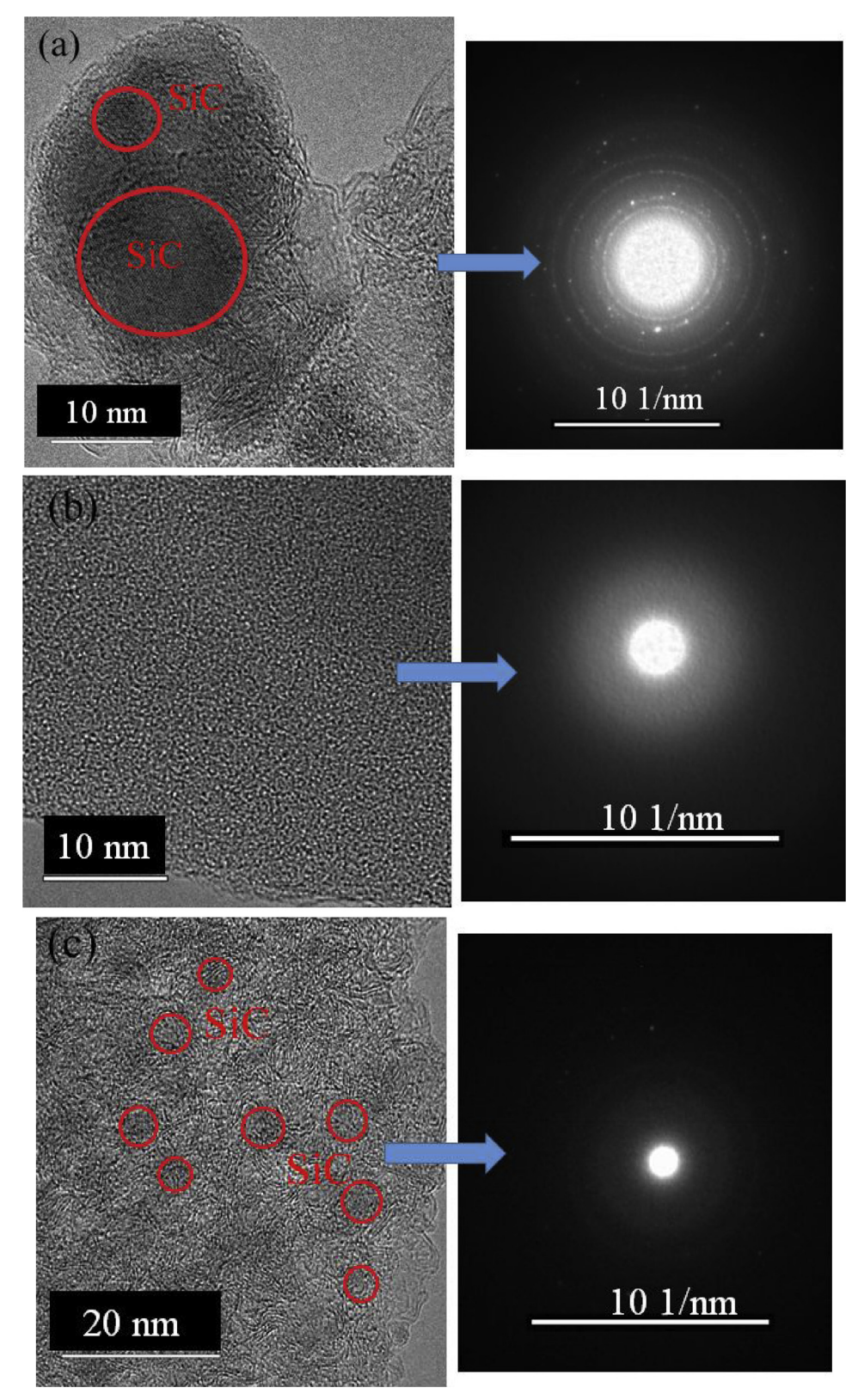


Fig. 3. Microstructures and diffraction patterns of: (a) flash pyrolyzed PMPS, (b) flash pyrolyzed Tospearl, and (c) traditionally pyrolyzed PMPS at 1400 °C. The red circles outline the profiles of the SiC crystallites. (For interpretation of the references to colour in this figure legend, the reader is referred to the web version of this article).

%. For the traditionally pyrolyzed Tospearl sample, it is 10.8 mol%. The significantly higher free carbon contents in the PMPS samples are a direct consequence of the C-rich precursor used.

As seen in Table 2, under the flash pyrolysis, slightly less free carbon

forms in the PMPS sample, which is consistent with the lower yield for the flash pyrolyzed PMPS sample (compared to the traditionally pyrolyzed sample) and indicates more carbon loss during the flash pyrolysis. For the Tospearl sample, flash pyrolysis leads to more free

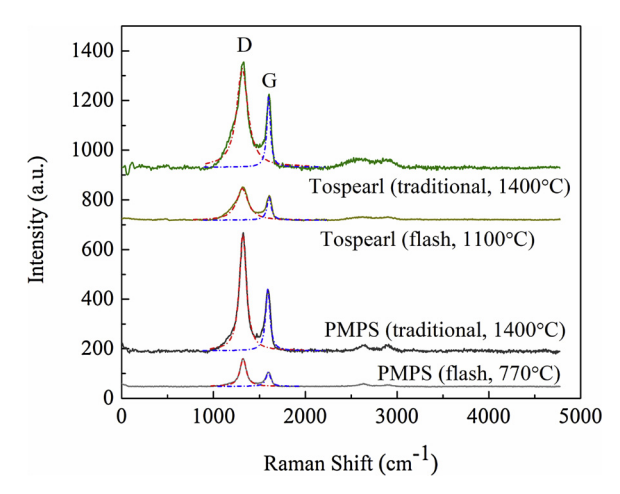


Fig. 4. Raman spectra for the flash pyrolyzed and traditionally pyrolyzed PMPS and Tospearl samples.

carbon formation under the flash pyrolyzed condition (less C-containing radical loss); thus, the ceramic yield is also higher.

The evolution of the free carbon phase can also be understood from Fig. 1. For both kinds of samples, the conductivity of the SiOC is determined by carbon. Before the flash event, the carbon phase exists in a disordered state. The flash temperatures correspond to the temperatures at which the free carbon phase begins to evolve significantly into ordered carbon, creating a percolating conductive network. For the PMPS sample, this percolating carbon formation temperature is 770 °C. For the Tospearl sample, the percolating carbon formation temperature is as high as 1100 °C. Since the internal pyrolysis temperatures at flash are about the same (1345 °C for the PMPS sample vs. 1342 °C for the Tospearl sample), the early formation of the percolating carbon (more ordered graphitic carbon) in the PMPS sample also means an earlier onset of SiC crystallization along with CO loss (Eq. (4)). For the Tospearl sample, the ordered carbon network forms at 1100 °C. The 'delayed' flash event allows carbon retention. However, the SiC formation is hindered due to the 'lack' of carbon.

Fig. 4 shows the Raman spectra of the flash pyrolyzed PMPS and Tospearl samples. Carbon can exist as either amorphous/disordered or ordered/graphitic, all of which can be determined using Raman spectroscopy. The D band at ~1350 cm⁻¹ is believed to arise from the defects and disordering in the free carbon, whereas the G band (in-plane vibrational mode) at 1588 cm⁻¹ is attributed to the ordered graphitic structure [38]. The broad G' band at 2682 cm⁻¹ and the weak band at 2934 cm⁻¹ can be assigned to a combination of the defective/disordered and graphitic modes (G + D). From our previous studies on flash pyrolysis, it is known that the ordering of the free carbon phase occurs as the amorphous carbon phase is rearranged into an ordered state [26]. The same ordering should occur for the carbon-rich PMPS while it is more limited in the Tospearl sample. Correspondingly, for the flash pyrolyzed PMPS sample the I_D/I_G ratio is 1.94, while for the flash pyrolyzed Tospearl sample it is 1.38. Theoretically, the C-rich PMPS sample should experience significant graphitization because of the readily available G phase; the relatively C-poor Tospearl sample should not experience significant graphitization because there is no conductive carbon phase in which electromigration can occur.

Based on the split peak area fitting results of Fig. 4, the amounts of ordered and disordered carbon for the flash pyrolyzed and traditionally pyrolyzed PMPS and Tospearl samples can be calculated as shown in Table 2. The PMPS sample has 36.5% disordered carbon at the flash pyrolysis condition and 39.4% at the traditional pyrolysis condition. The Tospearl sample, on the other hand, has 12.9% disordered carbon at the flash pyrolysis condition and 8.8% at the traditional pyrolysis condition. At the same time, the PMPS sample has 13.8% graphitic carbon at the flash pyrolysis condition and 13.3% at the traditional

pyrolysis condition while the Tospearl sample has 3.3% graphitic carbon at the flash pyrolysis condition and 2.2% at the traditional pyrolysis condition. Fundamentally, the higher graphitic carbon content should lead to earlier and easier flash event and the higher disordered carbon content should be more beneficial for SiC formation. This explains why the flash event happens at a much lower temperature for the PMPS sample while the SiC formation is also more obvious.

3.4. Phase contents based on Gibbs free energy minimization

As mentioned, for the PMPS and Tospearl samples, the total $\mathrm{SiO_aC_b}$ composition can be separated into $SiO_aC_b=f_c\cdot C+(1-f_c)\cdot SiO_xC_y$. The remaining $\mathrm{SiO_xC_y}$ phase separates along the $\mathrm{SiO_2}\text{-SiC}$ tie-line in the C-SiC-SiO₂ composition triangle. The compositions along the $\mathrm{SiO_2}\text{-SiC}$ tie-line can also be represented as $SiO_{(4-i)/2}C_{i/4}$, where $\mathrm{i}=0$ –4. Eq. (5) shows the phase separation reaction of $\mathrm{SiO_xC_y}$, where $\mathrm{f_0}$, $\mathrm{f_1}$, $\mathrm{f_2}$, $\mathrm{f_3}$ and $\mathrm{f_4}$ represent the amount of the corresponding phases.

$$SiO_{x}C_{y} = \sum_{i=0}^{4} f_{i}(SiO_{(4-i)/2}C_{i/4}) = f_{o} \cdot (SiO_{2}) + f_{1} \cdot \left(SiO_{\frac{3}{2}}C_{\frac{1}{4}}\right) + f_{2}$$

$$\cdot \left(SiOC_{\frac{1}{2}}\right) + f_{3} \cdot \left(SiO_{\frac{1}{2}}C_{\frac{3}{4}}\right) + f_{4} \cdot (SiC)$$
(5)

The overall Gibbs free energy of the phase separated amorphous SiO_xC_y system can be represented using the conventional formula:

$$G^{am-SiOC} = \sum_{i=0}^{4} f_i(T) \cdot G_i(T) + RT \sum_{i=0}^{4} f_i(T) \cdot \log f_i(T)$$
(6)

The stable phase contents of a given SiO_xC_y system depend on the minimum total Gibbs free energy ($G^{am-SiOC}$). The Gibbs free energy of the crystalline phases can be obtained using available data for SiC [39] and cristobalite [40]. Then the Gibbs free energy for the amorphous counterparts can be calculated based on:

$$G^{amorphous}(T) = G^{crystalline}(T) + \Delta E$$
 (7)

where ΔE is the vitrification enthalpy. ΔE for SiC, SiO₂, and C are 54 kJ/mol [41], 6.9 kJ/mol [42], and 20.8 kJ/mol [43], respectively. Thus, $G^{am-SiO_2}(T)$ or $G_0(T)=G^{cr-SiO_2}+6.9$ kJ/mol and $G^{am-SiC}(T)$ or $G_4(T)=G^{cr-SiC}(T)+54$ kJ/mol [40]. The phase contents for the PMPS and Tospearl samples can be calculated using Mathematica as shown in Table 3. The detailed Mathematica codes are provided in the supplement.

Table 3 shows that the flash pyrolyzed PMPS sample has significantly more SiO_2 and $SiO_{3/2}C_{1/4}$ phases and much lower $SiOC_{1/2}$ and SiO_{1/2}C_{3/4} phases compared to the traditionally pyrolyzed sample. For the Tospearl sample, this change is less obvious; since there is not as much free carbon available to react and form SiC, the microstructure will still contain predominantly Si-rich phases. The reason that the flash pyrolyzed samples have more Si-rich phases and less C-rich phases is believed to be due to the formation of more well-ordered carbon domains (graphitic carbon) during the fast flash process, which prevents silicon diffusion and reaction with amorphous (disordered) carbon to form C-rich tetrahedrals or SiC. In addition, the sudden temperature drop with the quick ending of the flash event intrinsically prevents silicon diffusion to carbon to form SiC. However, both Figs. 2 and 3 indicate more developed SiC crystallites in the flash pyrolyzed PMPS samples. This can be due to the better co-mixing state of localized silicon and carbon at the low temperature of flash, 770 °C, followed by the extremely fast heating rate from Joule heating. When the sample quickly heats up from this initial state, localized silicon and carbon can

Surprisingly, the SiC amounts for the PMPS and Tospearl samples are very similar at each pyrolysis condition (Table 3) even though based on Figs. 2 and 3 the SiC phase can be more easily detected for the PMPS samples, especially at the flash pyrolysis condition. This discrepancy can be explained by the better SiC crystallinity and/or larger SiC

crystallite size for the PMPS samples as explained earlier. It also means that the Gibbs energy minimization model is too idealized as it is only based on the thermodynamic data without considering the SiC crystallite size and phase development kinetics. This issue can be especially the case when the phase amount is low (such as for SiC).

4. Conclusions

In this study, flash and traditional pyrolysis studies were conducted for two different polysiloxane precursors: C-rich PMPS and less C-rich Tospearl. The flash event occurs at a much lower temperature for the PMPS sample than for the Tospearl sample. SiC crystallization is only observed for the PMPS sample. Both can be attributed to the carbonrich nature of the PMPS precursor. The carbon content and type have been quantified to illustrate the phase evolution difference. Using a Gibbs energy minimization approach, different phase amounts in the pyrolyzed samples can be calculated. On a relative basis, the PMPS samples have more C-rich tetrahedrals $(OC_{\frac{1}{2}}$ and $SiO_{\frac{1}{2}}C_{\frac{3}{4}})$ and the Tospearl samples have more Si-rich tetrahedrals such as SiO_2 and $SiO_{\frac{3}{2}}C_{\frac{1}{4}}$. Flash pyrolysis leads to more Si-rich phase formation for the C-rich PMPS precursor.

Declarations of interest

None.

Acknowledgments

We acknowledge the financial support from National Science Foundation under grant number CMMI-1634325 and Department of Energy under grant number DE-NE0008807.

Appendix A. Supplementary data

Supplementary material related to this article can be found, in the online version, at doi:https://doi.org/10.1016/j.jeurceramsoc.2019.03.051.

References

- [1] P. Colombo, G. Mera, R. Riedel, G.D. Soraru, Polymer-derived ceramics: 40 years of research and innovation in advanced ceramics, J. Am. Ceram. Soc. 93 (7) (2010) 1805–1837.
- [2] G.D. Soraru, G. Dandrea, R. Campostrini, F. Babonneau, G. Mariotto, Structural characterization and high-temperature behavior of silicon oxycarbide classes prepared from sol-gel precursors containing Si-H bonds, J. Am. Ceram. Soc. 78 (2) (1995) 379–387.
- [3] G.D. Soraru, S. Modena, E. Guadagnino, P. Colombo, J. Egan, C. Pantano, Chemical durability of silicon oxycarbide glasses, J. Am. Ceram. Soc. 85 (6) (2002) 1529–1536.
- [4] S. Walter, G.D. Soraru, H. Brequel, S. Enzo, Microstructural and mechanical characterization of sol gel-derived Si-O-C glasses, J. Eur. Ceram. Soc. 22 (13) (2002) 2389–2400.
- [5] P. Dibandjo, S. Dire, F. Babonneau, G.D. Soraru, New insights into the nanostructure of high-C SiOC glasses obtained via polymer pyrolysis, Glass Technol. Eur. J. Glass Sci. Technol. Part A 49 (4) (2008) 175–178.
- [6] H. Brequel, J. Parmentier, G.D. Soraru, L. Schiffini, S. Enzo, Study of the phase separation in amorphous silicon oxycarbide glasses under heat treatment, Nanostruct. Mater. 11 (6) (1999) 721–731.
- [7] S. Dire', M. Oliver, G.D. Soraru, Effect of Polymer Architecture on the Formation of Si-O-C Glasses, Innovative Processing and Synthesis of Ceramics, Glasses, and Composites II 94 (1999), pp. 251–261.
- [8] V.S. Pradeep, M. Graczyk-Zajac, R. Riedel, G.D. Soraru, New insights in to the lithium storage mechanism in polymer derived SiOC anode materials, Electrochim. Acta 119 (2014) 78–85.
- [9] H. Brequel, S. Enzo, S. Walter, G.D. Soraru, R. Badheka, F. Babonneau, Structure/ property relationship in silicon oxycarbide glasses and ceramics obtained via the sol-gel method, Metastable, Mech. Alloyed Nanocryst. Mater. 386-3 (2002) 359–364.
- [10] H. Brequel, J. Parmentier, S. Walter, R. Badheka, G. Trimmel, S. Masse, J. Latournerie, P. Dempsey, C. Turquat, A. Desmartin-Chomel, L. Le Neindre-Prum, U.A. Jayasooriya, D. Hourlier, H.J. Kleebe, G.D. Soraru, S. Enzo, F. Babonneau, Systematic structural characterization of the high-temperature behavior of nearly

- stoichiometric silicon oxycarbide glasses, Chem. Mater. 16 (13) (2004) 2585–2598.

 [11] R. Pena-Alonso, G. Mariotto, C. Gervais, F. Babonneau, G.D. Soraru, New insights on the high-temperature nanostructure evolution of SiOC and B-doped SiBOC polymer-derived glasses, Chem. Mater. 19 (23) (2007) 5694–5702.
- [12] H.J. Kleebe, C. Turquat, G.D. Soraru, Phase separation in an SiCO glass studied by transmission electron microscopy and electron energy-loss spectroscopy, J. Am. Ceram. Soc. 84 (5) (2001) 1073–1080.
- [13] C. Turquat, H.J. Kleebe, G. Gregori, S. Walter, G.D. Soraru, Transmission electron microscopy and electron energy-loss spectroscopy study of nonstoichiometric silicon-carbon-oxygen glasses, J. Am. Ceram. Soc. 84 (10) (2001) 2189–2196.
- [14] R.X. Ma, K. Lu, D. Erb, Effect of solvent in preparation of SiOC bulk ceramics, Mater. Chem. Phys. 218 (2018) 140–146.
- [15] D. Erb, K. Lu, Effect of additive structure and size on SiO₂ formation in polymerderived SiOC ceramics, J. Am. Ceram. Soc. 101 (12) (2018) 5378–5388.
- [16] D. Erb, K. Lu, Effects of SiO₂-forming additive on polysiloxane derived SiOC ceramics, Microporous Mesoporous Mater. 266 (2018) 75–82.
- [17] D. Erb, K. Lu, Additive and pyrolysis atmosphere effects on polysiloxane-derived porous SiOC ceramics, J. Eur. Ceram. Soc. 37 (15) (2017) 4547–4557.
- [18] J.K. Li, K. Lu, Highly porous SiOC bulk ceramics with water vapor assisted pyrolysis, J. Am. Ceram. Soc. 98 (8) (2015) 2357–2365.
- [19] M. Cologna, B. Rashkova, R. Raj, Flash sintering of nanograin zirconia in < 5 s at 850 degrees C, J. Am. Ceram. Soc. 93 (11) (2010) 3556–3559.
- [20] M. Cologna, J.S.C. Francis, R. Raj, Field assisted and flash sintering of alumina and its relationship to conductivity and MgO-doping, J. Eur. Ceram. Soc. 31 (15) (2011) 2827–2837
- [21] M. Cologna, A.L.G. Prette, R. Raj, Flash-sintering of cubic yttria-stabilized zirconia at 750 degrees C for possible use in SOFC manufacturing, J. Am. Ceram. Soc. 94 (2) (2011) 316–319.
- [22] J.S.C. Francis, R. Raj, Influence of the field and the current limit on flash sintering at isothermal furnace temperatures, J. Am. Ceram. Soc. 96 (9) (2013) 2754–2758.
- [23] J.S.C. Francis, R. Raj, Flash-sinterforging of nanograin zirconia: field assisted sintering and superplasticity, J. Am. Ceram. Soc. 95 (1) (2012) 138–146.
- [24] R. Raj, Joule heating during flash-sintering, J. Eur. Ceram. Soc. 32 (10) (2012) 2293–2301.
- [25] R. Raj, Analysis of the power density at the onset of flash sintering, J. Am. Ceram. Soc. 99 (10) (2016) 3226–3232.
- [26] R.X. Ma, D. Erb, K. Lu, Flash pyrolysis of polymer-derived SiOC ceramics, J. Eur. Ceram. Soc. 38 (15) (2018) 4906–4914.
- [27] L.X. Wang, K. Lu, Phase development of silicon oxycarbide nanocomposites during flash pyrolysis, J. Mater. Sci. 54 (8) (2019) 6073–6087.
- [28] B. Wang, D.E. Wolfe, M. Terrones, M.A. Haque, S. Ganguly, A.K. Roy, Electro-graphitization and exfoliation of graphene on carbon nanofibers, Carbon 117 (2017) 201–207
- [29] M.A. Mazo, A. Tamayo, A.C. Caballero, J. Rubio, Electrical and thermal response of silicon oxycarbide materials obtained by spark plasma sintering, J. Eur. Ceram. Soc. 37 (5) (2017) 2011–2020.
- [30] P. Miranzo, C. Ramírez, B. Román-Manso, L. Garzón, H.R. Gutiérrez, M. Terrones, C. Ocal, M.I. Osendi, M. Belmonte, In situ processing of electrically conducting graphene/SiC nanocomposites, J. Eur. Ceram. Soc. 33 (10) (2013) 1665–1674.
- [31] K. Lu, D. Erb, Additive and Pyrolysis Atmosphere Effects On High Surface Area Silicon Oxycarbides, Frontiers In Materials Processing Applications, Research and Technology, Bordeaux, France, 2017.
- [32] J. Li, K. Lu, T. Lin, F. Shen, Preparation of micro-/mesoporous SiOC bulk ceramics, J. Am. Ceram. Soc. 98 (6) (2015) 1753–1761.
- [33] M. Narisawa, S. Watase, K. Matsukawa, T. Dohmaru, K. Okamura, White Si-O-C(-H) particles with photoluminescence synthesized by decarbonization reaction on polymer precursor in a hydrogen atmosphere, Bull. Chem. Soc. Jpn. 85 (6) (2012) 724–726.
- [34] H. Yoshida, Y. Sakka, T. Yamamoto, J.M. Lebrun, R. Raj, Densification behaviour and microstructural development in undoped yttria prepared by flash-sintering, J. Eur. Ceram. Soc. 34 (4) (2014) 991–1000.
- [35] J. Cordelair, P. Greil, Electrical conductivity measurements as a microprobe for structure transitions in polysiloxane derived Si-O-C ceramics, J. Eur. Ceram. Soc. 20 (12) (2000) 1947–1957.
- [36] K. Lu, Porous and high surface area silicon oxycarbide-based materials-a review, Mater. Sci. Eng. R. 97 (2015) 23–49.
- [37] G.D. Soraru, R. Pena-Alonso, M. Leoni, C-rich micro/mesoporous Si(B)OC: in situ diffraction analysis of the HF etching process, Microporous Mesoporous Mater. 172 (2013) 125–130.
- [38] J.M. Pan, J.F. Pan, X.N. Cheng, X.H. Yan, Q.B. Lu, C.H. Zhang, Synthesis of hierarchical porous silicon oxycarbide ceramics from preceramic polymer and wood biomass composites, J. Eur. Ceram. Soc. 34 (2) (2014) 249–256.
- [39] J.A. Golczewski, F. Aldinger, Thermodynamic modeling of amorphous Si-C-N ceramics derived from polymer precursors, J. Non-Cryst. Solids 347 (1-3) (2004)
- [40] M.W. Chase Jr., NIST-JANAF Thermochemical Tables, Fourth Edition, American Chemical Society; New York: American Institute of Physics for the National Institute of Standards and Technology, Washington, DC, 1998.
- [41] G. Foti, Silicon carbide: from amorphous to crystalline material, Appl. Surf. Sci. 184 (1) (2001) 20–26.
- [42] K. Tapasa, T. Jitwatcharakomol, Thermodynamic calculation of exploited heat used in glass melting furnace, Procedia Eng. 32 (2012) 969–975.
- [43] A.H. Tavakoli, M.M. Armentrout, M. Narisawa, S. Sen, A. Navrotsky, White Si-O-C ceramic: structure and thermodynamic stability, J. Am. Ceram. Soc. 98 (1) (2015) 242–246.